Received: 5 April 2019 | Accepted: 26 October 2019
DOI: 10.1111/pce.13672

ORIGINAL ARTICLE

WILEY Plant, Cell & Environment

Comparative metabolomics implicates threitol as a fungal signal supporting colonization of *Armillaria luteobubalina* on eucalypt roots

Johanna W.-H. Wong[1] | Krista L. Plett[1] | Siria H.A. Natera[2] | Ute Roessner[2,3] | Ian C. Anderson[1] | Jonathan M. Plett[1]

[1] Hawkesbury Institute for the Environment, Western Sydney University, Richmond, Sydney, Australia

[2] Metabolomics Australia, The University of Melbourne, Parkville, Melbourne, Australia

[3] School of BioSciences, The University of Melbourne, Parkville, Melbourne, Australia

Correspondence
Jonathan M Plett, Hawkesbury Institute for the Environment, Western Sydney University, Richmond NSW 2753, Australia.
Email: j.plett@westernsydney.edu.au

Funding information
Australian Plants Society, Grant/Award Number: Valette Williams Scholarship in Botany; Western Sydney University, Grant/Award Number: PhD Research Scholarship; Australian Research Council, Grant/Award Number: DE150100408

Abstract

Armillaria root rot is a fungal disease that affects a wide range of trees and crops around the world. Despite being a widespread disease, little is known about the plant molecular responses towards the pathogenic fungi at the early phase of their interaction. With recent research highlighting the vital roles of metabolites in plant root–microbe interactions, we sought to explore the presymbiotic metabolite responses of *Eucalyptus grandis* seedlings towards *Armillaria luteobuablina*, a necrotrophic pathogen native to Australia. Using a metabolite profiling approach, we have identified threitol as one of the key metabolite responses in *E. grandis* root tips specific to *A. luteobubalina* that were not induced by three other species of soil-borne microbes of different lifestyle strategies (a mutualist, a commensalist, and a hemi-biotrophic pathogen). Using isotope labelling, threitol detected in the *Armillaria*-treated root tips was found to be largely derived from the fungal pathogen. Exogenous application of D-threitol promoted microbial colonization of *E. grandis* and triggered hormonal responses in root cells. Together, our results support a role of threitol as an important metabolite signal during eucalypt-*Armillaria* interaction prior to infection thus advancing our mechanistic understanding on the earliest stage of *Armillaria* disease development.

KEYWORDS

biomarkers, disease detection, fungal tree pathogen, GC-MS, metabolomics, plant–microbial interaction, rhizosphere, soil microbes

1 | INTRODUCTION

Armillaria root disease is a ubiquitous root disease threatening numerous tree species in the world including a wide range of eucalypt species. *Armillaria*-infected eucalypts usually show symptoms such as white mycelical sheets under the bark, white rot of sapwood, black rhizomorphs penetrating root surfaces, and honey-coloured mushrooms clusters. Further aboveground symptoms include reduced growth of the host, distress cone crop, and crown thinning (Kile, 2000). As *Armillaria* usually causes only a minor disturbance to native eucalypts forests and plantations, these fungi are often considered as an unimportant, indigenous soil-borne pathogen of eucalypts in Australia (Burgess & Wingfield, 2004). However, when trees are under stress due to drought or temperature extremes, they became more prone to *Armillaria* disease (Sturrock et al., 2011). Therefore, in view of changing global climatic conditions, root rot attributed to *Armillaria* infection could become more prominent in the future.

Within the *Armillaria* genus, *Armillaria luteobubalina* is a particularly deadly species that can cause root rot or even mortality among eucalypts in both native forests and plantations, setting itself apart from other native *Armillaria* species in Australia (Burgess & Wingfield, 2004; Kile, 2000). *A. luteobubalina* has been the major causal agent of dieback and decline of eucalypts in central Victoria and south-western Australia in the last century (Kile, 1981; Robinson, 2003). The current diagnostic strategy for *Armillaria* disease relies heavily on visual inspection for the symptoms mentioned above, which are unfortunately similar to other root diseases and usually only appear in the later stage of the disease, making *Armillaria* disease difficult to detect (Kile, 2000). Despite being a common tree disease, little is known about the molecular pathways underlying the *Armillaria* disease development in eucalypts—knowledge that could be critical to devising new methods for control of *Armillaria* root infection. Transcriptomic analysis of *Armillaria* after colonization of grand fir (Ross-Davis et al., 2013) and genomic and proteomic analysis of *A. mellea* (Collins et al., 2013) have explored the contribution of digestive enzymes and effector proteins during degradation of the plant tissues, yet the molecular mechanisms initiating the infection of *Armillaria* fungi on tree roots are largely unknown. Better knowledge concerning the onset of *Armillaria* infection in trees could aid more effective, proactive management of the disease.

Interactions between plants and soil microbes are often initiated by the exchange of metabolite signals. Whereas the majority of metabolites used as signals between organisms in plant-microbe interactions are common to both mutualistic and pathogenic symbioses (Wong et al., 2019; Xu et al., 2015), there are also examples in the literature where either soil microbes or their plant hosts release genus- or species-specific metabolites that facilitate their interaction. For example, root exudate contents of tomato and tall fescue vary based on the type of soil-microbes with which they were interacting (Guo, McCulley, & McNear, 2015; Kamilova, Kravchenko, Shaposhnikov, Makarova, & Lugtenberg, 2006). Similarly, soil-microbes can produce specific metabolites to facilitate root colonization on host plants; the secretion of hypaphorine by the ectomycorrhizal fungus *Pisolithus tinctorius* is related to colonization (Beguiristain & Lapeyrie, 1997). These studies are, therefore, a proof of concept demonstrating that a range of metabolites derived from either the plant or the interacting microbe can be selectively present during plant–microbial interaction. Further, these studies may indicate that the difference in plant metabolite responses towards different microbes could be the key to determine the interaction outcome between the two organisms. Given their key importance, these metabolite responses could also be used as "biomarkers" to indicate the health or disease status in plants and provide further insight into the pathogenicity of the disease agent. Using gas chromatography-coupled mass spectrometry (GC-MS), metabolite biomarkers have been identified for plant diseases such as Tomato yellow leaf curl virus (Sade et al., 2014), *Ganoderma* disease in oil palm (Nusaibah, Siti Nor Akmar, Idris, Sariah, & Mohamad, 2016), and *Fusarium* infection in maize (Sherif et al., 2016). For *Armillaria* disease, pine seedlings infected with *Armillaria ostoyae* exhibited distinct levels of certain metabolites 9-month post-inoculation despite there being no visible symptoms (Isidorov, Lech, Żółciak, Rusak, & Szczepaniak, 2008). To further expand our knowledge of the mechanisms regulating *Armillaria* pathogenicity and to advance the detection strategy of *Armillaria* root rot, we need to improve our understanding of the host metabolite responses, and their underlying roles, during the early stages of the interaction.

In this study, we explore the metabolite response of *Eucalyptus grandis* roots towards *A. luteobubalina* during the earliest phases of interaction (i.e., presymbiosis) in an effort to advance our understanding of key metabolite signals underpinning the onset of *Armillaria* disease in eucalypts. The root metabolite responses towards *A. luteobubalina* at 24-hr presymbiotic interaction (i.e., before the plants and fungi come into physical contact) were profiled and compared with the metabolite profiles of eucalypt roots similarly exposed to three other distinct groups of microbes—the mutualistic ectomycorrhizal fungus *Pisolithus microcarpus*; the commensal fungus *Suillus granulatus*, and the hemi-biotrophic oomycete *Phytophthora cinnamomi*, in order to identify metabolite responses that are specific to the *E. grandis*–*A. luteobubalina* interaction. We identify a number of metabolite responses specific to the *Armillaria* interaction. We further characterize the role of one of these metabolites, D-threitol, on *E. grandis* defence gene expression and on *Armillaria* infection efficiency.

2 | MATERIALS AND METHODS

2.1 | Fungal culture condition

A total of 10 different isolates of fungi corresponding to three fungal species representing different lifestyles and one isolate of pathogenic oomycete *P. cinnamomi* were sampled from several locations in New South Wales, Australia and used in this study (Table S1). Agar plugs containing mycelium of each fungal isolates and oomycete isolate were grown on a piece of permeable, sterile cellophane membrane (Kleerview Covers by Fowlers Vacola Manufacturing Co Ltd.) in their preferred growth medium (Table S1). The fungal and oomycete cultures were allowed to grow in a dark growth cabinet controlled at 25°C for 14 days before the presymbiosis experiment with *E. grandis*.

2.2 | Plant growth condition

To establish the experiment, *E. grandis* seeds (seedlot 20974) were obtained from the Commonwealth Scientific and Industrial Research Organisation (Clyton, Victoria, Australia) tree seed centre. Seeds sterilization was performed by submerging the seeds in 30% (v/v) H_2O_2 for 10 min followed by washing in sterilized deionized water for 5 min five times. After sterilization, seeds were germinated in 1% water agar for 3 weeks before transferring into half-strength Modified Melin-Norkrans (MMN) medium. The *E. grandis* seedlings were cultivated in a controlled growth chamber (22–30°C; 16-hr light cycle) for 1 month prior to the presymbiotic interaction with microbes.

2.3 | Presymbiotic plant–microbial interaction set-up for untargeted metabolite profiling

Both *E. grandis* seedlings, fungal cultures, and oomycete cultures were allowed to acclimatize to modified half-strength MMN media without glucose for 3 days before the set-up of the presymbiotic interaction. At the beginning of the experiment, each cellophane membrane containing the fungal/oomycete mycelia was placed on top of the root system of a *E. grandis* seedling (2-month-old) whereby the cellophane membrane physically separated the fungal/oomycete mycelia from the *E. grandis* root system but allowed diffusion of chemical compounds between the microbe and the plant as per Wong et al. (2019). The 24-hr presymbiotic interaction was carried out in a controlled growth chamber (22–30°C; 16-hr light cycle), and root tips of *E. grandis* were sampled, subjected to snap-freezing with liquid N_2 and stored in a −80°C freezer. An untreated seedling control was also set up (*E. grandis* seedlings covered by sterile cellophane membrane). The frozen samples were sent to Metabolomics Australia at the University of Melbourne for untargeted metabolite profiling using GC-MS as described in Roessner et al. (2001). Details of the sample preparation and analytical procedures are described in supplementary materials and methods. Although GC-MS is not able to comprehensively profile the full suite of metabolites within the root, it has the advantage of a high efficiency of peak separation and reproducible retention times that enable it to be better compared with previously performed research (Scalbert et al., 2009; Vinaixa et al., 2016). The ionization used in the method also allows for standardized spectral fingerprints that increase the possibility of positive identification against public databases. Conversely, the derivatization steps required for the analysis mean that some compounds become too unstable and are therefore missed. Other techniques could be used to generate a longer list of molecular features, but as the aim of this paper was to find a method that could be used comparably between laboratories and use as simple a workflow as possible, thereby increasing the possible implementation as a potential screening tool for disease in different settings, we chose to use the GC-MS platform.

2.4 | Soil-based *Armillaria*-treatment set up for untargeted metabolite profiling

Two-month-old *E. grandis* seedlings growing on half-strength MMN media were transferred individually into pots containing soil (Osmocote professional seed and cutting potting mix by Evergreen Garden Care Australia Pty Ltd.) sterilized by autoclaving two times at 121°C for 3 hr. The seedlings were then allowed to grow in soil for another month in a growth chamber (22–30°C; 16-hr light cycle). To allow soil-based interaction with *A. luteobubalina*, the 3-month-old *E. grandis* seedlings were transferred into a pot with 0.5 L of soil inoculated with 25 ml of homogenized *A. luteobubalina* culture in potato dextrose agar (PDA) media. An uninoculated control (0.5 L soil mixed with 25 ml of sterile PDA media) was also set up. After 7 days of interaction in the abovementioned growth chamber, the soil was discarded from the pot and the root tips of the *E. grandis* seedlings were harvested and immediately frozen in liquid N_2. The frozen root tip samples were analysed for metabolite profiles as above.

2.5 | Targeted D-threitol quantification throughout *A. luteobubalina* colonization of *E. grandis* and under different nutrient regimes

In order to understand the production of threitol throughout colonization, *E. grandis* and *A. luteobubalina* were grown separately and pretreated as above. Fungal cultures were then placed into either indirect contact with *E. grandis* roots for 24 hr, as described above, or were placed into direct physical contact. For the latter samples, at prescribed intervals (24 hr, 48 hr, 1 week, and 2 weeks) the roots and adherent fungi were separated and snap frozen in liquid nitrogen and stored at 80°C until extraction and analysis. In order to understand if nutrient levels in the growth medium may serve as a signal for threitol production, we grew *A. luteobubalina* on a series of media with decreasing concentrations of potato dextrose (1x, 1/2x, 1/4x, and 1/10x) for 2 months after which fungal tissue samples were taken, snap frozen, and then analysed for threitol concentration as below.

Because of different extraction efficiencies, we used two different methods to extract threitol from roots and from fungi. For the roots, the fresh weight of the root tip samples were recorded during harvest. Approximately 20–30 mg of frozen root samples per biological replicate were homogenized using a bead mill (FastPrep-24, MP Biomedicals, LLC) and then incubated with 600 µl of 60% (v/v) methanol (high-performance liquid chromatography [HPLC] grade) in a thermomixer (Eppendorf) set at 60°C with a mixing speed of 1,000 rpm for 30 min. The extracts were then centrifuged at 13,000 rpm for 5 min. Cleared supernatant samples were then collected and dried using a vacuum concentrator (SpeedVac, Thermo Fisher Scientific) set at ambient temperature. The dried extracts were resuspended in 1/10 of the original volume of 60% (v/v) methanol and stored at −20°C until analysis. For the fungal samples, the fresh weight of the fungal mycelia samples were recorded during harvest. Frozen fungal samples were homogenized using a bead mill (FastPrep-24, MP Biomedicals, LLC) and then incubated with 100 µl per 10 mg fresh sample of pure methanol (HPLC grade) in a thermomixer (Eppendorf) set at 30°C with a mixing speed of 1,000 rpm for 15 min. The methanol extracts were then centrifuged at 13,000 rpm for 5 min. Clarified supernatant samples were then collected and set aside in a new microcentrifuge tube. 100 µl per 10 mg fresh samples of deionized water was added into the sample pellet, vortexed for 10 s and incubated at ambient temperature for 5 min. The water extracts were then centrifuged at 13,000 rpm for 5 min. Clarified water extracts were collected and mixed with the aforementioned methanol extracts and dried using a vacuum concentrator (SpeedVac, Thermo Fisher Scientific) set at ambient temperature. The dried extracts were resuspended in 1/5 of the original volume of 50% (v/v) methanol and stored at 20°C until analysis.

Of each sample, 2 µl was injected into the Agilent 1260 Infinity HPLC-system equipped with a Shodex Asahipak NH2P-50 4E column

(4.6 × 250 mm, 5 μm) warmed at 55°C, and a Dionex Corona charged aerosol detector. The mobile phase was optimized based on the sample types. Elution was done isocratically with 1:1 (v/v) deionized water: acetonitrile (HPLC grade) for root samples, whereas 1:4 (v/v) deionized water: acetonitrile (HPLC grade) was used for fungal samples. In both cases, the elution was done at the rate of 1.2 ml/min for 10 min. A set of seven D-threitol standards at concentrations ranging from 250 ppm to 4,000 ppm were used to identify and quantify the concentration of threitol in each sample. The resulting quantitation was normalized based on the fresh weight of each sample.

2.6 | Statistical analysis of metabolite profiling data

The metabolite profiling data matrix, containing the relative response ratios of each metabolite (including both identified and unknown metabolites) in each condition, was loaded on the R platform (Version 3.5.1). Data transformation (log-transformation and auto-scaling), univariate analysis, and principle component analysis were performed with MetaboAnalystR (Version 1.0.1) with the metabolite profiling data matrix. Recursive partitioning and regression tree and parallel random forest were performed using the caret package (Version 6.0-81), whereas sparse partial least square-discriminative analysis was carried out with mixOmics (Version 6.6.0) package on R. The workflow of this analysis can be found in Figure S1.

2.7 | Threitol quantitation, ^{13}C-isotopic labelling, and tracing

Prior to presymbiotic interaction with *E. grandis*, *A. luteobubalina* and *P. microcarpus* were labelled with ^{13}C by growing the fungi on modified half-strength MMN agar media with 1 g/L of 99% $^{13}C_6$-glucose (Cambridge Isotope Laboratories, Inc.) for 1 month. An unlabelled control was also prepared. The fungal cultures were then transferred to half-strength MMN media (without glucose) for 3 days, followed by presymbiotic interaction with *E. grandis* seedlings for 24 hr as described above. Root tip samples and fungal mycelia were collected and snap-frozen in liquid N_2 and subsequently stored in −80°C freezer until extraction and metabolite analysis by Metabolomics Australia at the University of Melbourne. Untargeted metabolite profiling, threitol ^{13}C isotope enrichment analysis, as well as targeted quantitation of threitol were performed as described in Roessner et al. (2001), Nanchen, Fuhrer, and Sauer (2007), and Dias et al. (2015), respectively. Detailed procedures can be found in supplementary materials and methods.

2.8 | Threitol treatment and microbial infection assay

To identify the impact of D-threitol on the rate of microbial infection, 1-month-old mycelia of *A. luteobubalina*, 1-week-old hyphae of *P. cinnamomi*, or 2-week-old mycelia of *P. microcarpus* isolate SI-14 were placed directly onto *E. grandis* roots on three types of half-strength MMN agar media with different D-threitol concentrations—0, 0.3, and 12 ppm, and cocultured for 14 days in a growth chamber set at the growth conditions described above. These D-threitol concentrations were chosen based on the quantified ranges of the metabolite in the roots of *E. grandis* across all of our experiments. Sterile *E. grandis* seedlings monoculture growing on media of the same threitol concentration was set up alongside as a negative control. After 14 days, the lateral roots were observed under a stereoscope and degree of infection/colonization were counted manually for *E. grandis* seedlings. Infection for the two pathogens was classified as the percentage of root lesions caused by either *A. luteobubalina* or *P. cinnamomi* divided by the total number of lateral roots in contact with fungal mycelium. For the mutualistic fungus *P. microcarpus* isolate SI-14, the percentage of colonized root tips was compared between each treatment.

2.9 | Electrolyte leakage

As a secondary means to quantify damage to the roots caused by *A. luteobubalina* over time, we measured electrolyte leakage of infected roots across the timecourse of colonization (i.e., from before contact through 2 weeks after contact). For these assays, two to four lateral roots in contact with *A. luteobubalina* were excised and placed in 3 ml of Milli-Q water and left to incubate at 25°C for 1 hr. After this incubation, the conductivity of the water was measured using a conductivity metre. The samples were then boiled at 95°C for 1 hr followed by cooling of the sample back to 25°C. Following temperature equilibration, conductivity was again measured and the percentage of the first reading versus the second reading was recorded. An average of four biological replicates were performed per data point.

2.10 | RNA extraction and RT-qPCR assay

E. grandis seedlings were transferred onto half-strength MMN agar media supplemented with 0 ppm or 12 ppm D-threitol. After 24 hr, the plant roots were harvested and three biological replicates from each condition were immediately frozen in liquid nitrogen. RNA was extracted from the roots with the Bioline Isolate II miRNA extraction kit. Extracted RNA was used as a template for complementary DNA (cDNA) synthesis using the Bioline SensiFAST cDNA synthesis kit. Real-time quantitative polymerase chain reaction (PCR; RT-qPCR) analysis was conducted on a BioRad CFX96 Touch RT-PCR cycler using the Bioline SensiFAST SYBR No-ROX kit. Log_2 fold change of gene expression of 12 ppm D-threitol treated roots as compared with control roots (0 ppm D-threitol) was calculated for the closest *E. grandis* homologues to known Arabidopsis hormone responsive genes: ABI3 (*Eucgr.H00815*), PIN1 (*Eucgr.K02271*), PIN2 (*Eucgr.C00078*), PIN3 (*Eucgr.B02902*), ARR16 (*Eucgr.G03141*), ARR6 (*Eucgr.B02571*), GA3ox1 (*Eucgr.F02568*), Myc2 (*Eucgr.E00277*), and VSP2 (*Eucgr.J02927*). RT-qPCR gene expression results were normalized using *Eucgr.C00350* and *Eucgr.B03031* as control genes. Primers used in the RT-qPCR assays are listed in the Table S2. To understand if the impact of D-threitol on the transcriptomic expression of these

hormone-responsive genes was specific to this compound or if it was a general response to different sugar compounds, we also exposed a second set of *E. grandis* seedlings to the sugar myo-inositol at either 0 or 25 ppm for 24 hr. RNA was then extracted from these root systems, followed by cDNA synthesis and RT-qPCR performed on the same genes as above.

3 | RESULTS

3.1 | Metabolite responses of *E. grandis* root tips during presymbiosis with *A. luteobubalina*

With GC-MS based untargeted metabolite profiling, a total of 117 metabolites were detected in *E. grandis* root tips when grown axenically, including 67 identifiable metabolites and 50 unknown metabolites (Table S3). After 24 hr of presymbiotic "indirect" contact with *A. luteobubalina* (i.e., plant and fungus were allowed to exchange diffusible signals but were physically separated by a membrane), 13 metabolites in *E. grandis* root tips were increased in abundance by more than twofold. Apart from the unknown metabolites, the highly repressed root metabolite responses (fold change <0.5) mostly belong to organic acids, whereas the majority of highly enriched metabolites (fold change >2) are either sugars, sugar alcohols, amines, or amino acids (Table 1; full list of root metabolite responses towards *A. luteobubalina* are listed in Table S4). Mannitol, trehalose, and threitol exhibited the most significant enrichment in *E. grandis* roots upon interaction with *A. luteobubalina* (Figure 1).

In order to understand which of the metabolite responses by *E. grandis* might be specific to contact with *A. luteobubalina*, we compared the *E. grandis* root metabolite responses described above with root metabolite responses to three other species of soil microbes commonly found in eucalypt forests in Australia, including the pathogenic oomycete *P. cinnamomi*; the commensal fungus *S. granulatus*; and the mutualistic ectomycorrhizal fungus, *P. microcarpus*. Principle component analysis could not clearly separate the metabolite profiles of *E. grandis* root tips based on the microbial treatment (Figure 2), although permutational multivariate analysis of variance indicated that the microbial treatments have significant effect on *E. grandis* root metabolite profiles ($p < .001$) whereby 20.58% of the variance in the metabolite responses can be explained by the different species of interacting microbes. Our results suggest that the overall metabolite responses of *E. grandis* roots are nonrandom and that certain root metabolites respond selectively towards different species of microbes.

3.2 | Identification of *Armillaria*-specific metabolite responses in *E. grandis* root tips

To identify potential metabolites in *E. grandis* root tips that are specific to the interaction with *A. luteobubalina*, we made use of supervised machine learning (ML) models. Three ML models—parallel random forest (parRF), sparse partial least square discriminative analysis (sPLSDA), and recursive partitioning and regression tree (rpart)—were trained with a subset of our metabolomics datasets ($n = 36$) to select important metabolite responses with high discriminative power that effectively split the root metabolite profiles into three groups as follows: *A. luteobubalina*-treated group (*Armillaria*), untreated control group (control), or other microbial treatments (other). The accuracy of each of the three ML models were evaluated by cross-validation and fine-tuning of parameters to optimize their performance (Table 2). Prediction performance of each model was validated externally with a subset of the data ($n = 12$) that was previously omitted for testing purposes (Table 2). With the area under receiver operating characteristic index approaching 1, the performance testing result ensured a high confidence was accrued by our ML models.

The top 10 important metabolite responses with the highest discriminative capacities were selected by each of the ML models (Figure 3a). Threonic acid, shikimic acid, threitol, lactic acid, and inositol were commonly selected by the three ML models as the most important features for classification between *Armillaria*, control, and other (Figure 3b). These three classification groupings could also be effectively separated when the responses of these important metabolites (threonic acid, shikimic acid, threitol, lactic acid, and inositol) were considered together (Figure 3c). Threitol was the only discriminatory metabolite induced in the *Armillaria* group but not the other groups, whereas the other four aforementioned metabolite responses were repressed in *Armillaria* and other in comparison with control (Figure 3b). In a separate targeted threitol quantitation analysis, we found that the quantity of D-threitol in root tips treated with *A. luteobubalina* was >20 times higher than in root tips treated with *P. microcarpus* (Table 3). Given the strong explanatory value of threitol from these results, we wished to see if it was also present in *E. grandis* root tips when they were exposed to *Armillaria* in a system that more closely resembled a natural system (i.e., a soil-based system). We found that the enrichment of threitol was also observed in *E. grandis* root tips in this soil-based setup, but only when *Armillaria* was present (Figure 4).

3.3 | Threitol detected in *E. grandis* root tips is largely of fungal origin

As we identified threitol to be significantly enriched on root tips when *E. grandis* interacts with *A. luteobubalina*, we sought to ascertain the origin of the threitol—whether it was a fungal-derived metabolite that diffused to *E. grandis* roots or a plant-synthesized metabolite. Therefore, we used an isotope-labelling experimental set-up to separate fungal-derived metabolites from plant-derived metabolites. By culturing *A. luteobubalina* on $^{13}C_6$-glucose spiked media for a month, we successfully enriched the proportion of ^{13}C-labelled threitol among all detectable isotopomers in the fungal mycelium, especially the $^{13}C_3$-threitol (derivative $m/z = 220$) and $^{13}C_4$-threitol (derivative $m/z = 221$) isotopomers (Figure 5). In these samples, ^{13}C-labelled isotopomers made up >55% of the total threitol abundance. In comparison, threitol, detected when *A. luteobubalina* was grown on a

TABLE 1 The highly regulated metabolite responses in *Eucalyptus grandis* root tips after 24 hr presymbiotic interaction with *Armillaria luteobuablina*

Metabolite	Metabolite class	Mean fold change	*p* value
Induced by *Armillaria luteobuablina*			
Threitol	sugars and sugar alcohols	18.80	.01*
Tartaric acid	organic acids	13.29	.09
Trehalose	sugars and sugar alcohols	11.29	.02*
Mannitol	sugars and sugar alcohols	8.26	.02*
Unknown_37 (*mz* = 231, *rt* = 20.0801)	unclassified	5.55	.01*
Unknown_50 (*mz* = 357, *rt* = 25.0806)	unclassified	2.96	.12
Unknown_34 (*mz* = 246, *rt* = 19.6291)	unclassified	2.29	.30
Ethanolamine	amino acids and amines	2.27	.09
Proline	amino acids and amines	2.22	.16
Unknown_28 (*mz* = 129, *rt* = 18.3399)	unclassified	2.22	.08
Phosphoric acid	other	2.13	.37
Unknown_52 (*mz* =333, *rt* = 25.2714)	unclassified	2.11	.05
Unknown_48 (*mz* = 333, *rt* = 24.8404)	unclassified	2.08	.04*
Repressed by *A. luteobubalina*			
Glyceric acid	organic acids	0.41	.00*
Unknown_49 (*mz* = 366, *rt* = 24.9799)	unclassified	0.41	.12
Gulonic acid	organic acids	0.41	.03*
Malic acid	organic acids	0.41	.04*
Unknown_65 (*mz* = 446, *rt* = 28.4172)	unclassified	0.37	.02*
Unknown_13 (*mz* = 173, *rt* = 12.4636)	unclassified	0.37	.01*
Unknown_35 (*mz* = 333, *rt* = 19.7161)	unclassified	0.35	.01*
Oxalic acid	organic acids	0.32	.00*
Unknown_26 (*mz* = 275, *rt* = 18.1341)	unclassified	0.29	.08
Shikimic acid	organic acids	0.28	.00*
Unknown_20 (*mz* = 159, *rt* = 16.6234)	unclassified	0.26	.05*
Pyroglutamic acid	amino acids and amines	0.20	.00*
Lactic acid	organic acids	0.14	.08
Threonic acid	organic acids	0.12	.00*

Note. Fold change is calculated in relation to un-inoculated control *Eucalyptus grandis* root tips.

*p value < .05.

substrate without ^{13}C enrichment, had a significantly lower percentage of ^{13}C-labelled isotopomers. When *E. grandis* root tips were placed into presymbiotic interaction with the ^{13}C-labelled *A. luteobubalina* mycelium, >40% of the total threitol recovered in the root tips was labelled with ^{13}C. These results demonstrate that *A. luteobubalina* is able to synthesize its own threitol and suggests that the majority of threitol detected *E. grandis* root tips during presymbiosis originated from *A. luteobubalina*.

3.4 | Threitol production occurs prior to cell damage and under nutrient-limited conditions

To gain insight into the production of D-threitol in *A. luteobubalina* during colonization of *E. grandis* and to understand the uptake of this compound in plant tissues in relation to disease progression, we quantified D-threitol in both the fungal tissues and the plant root across colonization. As shown in Figure 6a, D-threitol was found in *A. luteobubalina* tissues at very high concentrations prior to contact when grown on glucose-free medium (i.e., time point "0") and for the first 24 hr of interaction between the two organisms be that presymbiotic interaction or direct plant–fungal contact. After 24 hr, fungal production of D-threitol began to significantly decrease until it reached its lowest detected concentration at 2-week post-contact with the host roots. In *E. grandis*, D-threitol root concentrations prior to the interaction with *A. luteobubalina* was near the detection limit of the machine (Figure 6a). These concentrations rose steadily through 24 hr of direct physical contact between the two organisms after which root-associated D-threitol decreased slightly, but maintained a higher than

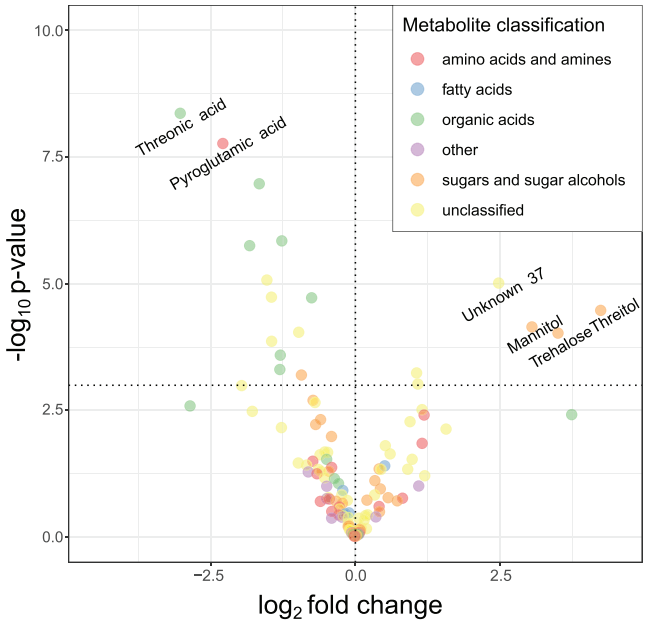

FIGURE 1 Volcano plot shows differential metabolite responses of *Eucalyptus grandis* root tips towards *Armillaria luteobubalina* presymbiotic interaction (n = 8) in comparison with untreated control root tips (n = 4). The x-axis and y-axis explain the $\log_2$-transformed fold change and the significance of the fold change in form of $-\log_{10}$ p value, respectively. Each point represents a type of metabolite detected by gas chromatography-coupled mass spectrometry untargeted metabolite profiling, with the colour of the points represent the classification of the metabolites. Significantly differential metabolite responses ($|\log_2$fold change$|$ > 2 and p value < .05) are labelled in the plot [Colour figure can be viewed at wileyonlinelibrary.com]

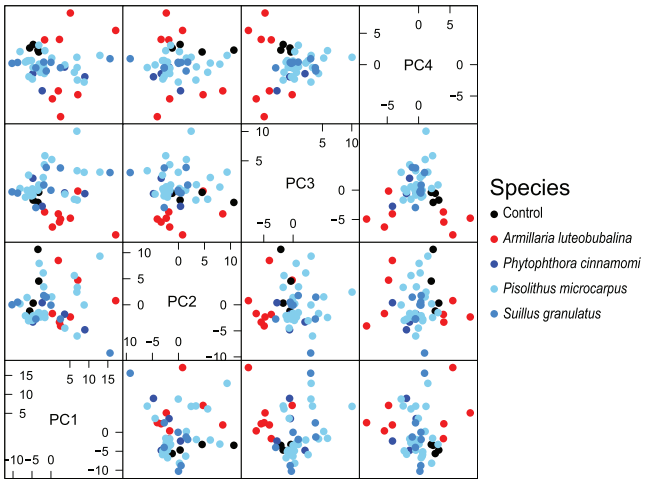

FIGURE 2 Scatter plot matrix demonstrates the dispersion of overall metabolite profiles for *Eucalyptus grandis* root tips under presymbiotic interaction with five distinct microbial species. The plot describes the correlation of the first four principle components (PCs) of the principal component analysis. Each point represents the metabolite profile of a *E. grandis* root tips sample, with the colour representing a different microbial treatment [Colour figure can be viewed at wileyonlinelibrary.com]

control level across fungal colonization of root tissues. It was interesting to note, based on the measurement of ion leakage as a proxy for cell damage, that whereas D-threitol accumulation in the fungus was at its highest, plant cell damage was at its lowest (Figure 6b). It was not until the 1 week time point and beyond that we observed significant increases in cell damage.

As D-threitol concentrations in fungal tissues was highest prior to extensive root damage, and because D-threitol concentration tailed off, whereas root damage increased, this led us to question whether D-threitol production may be controlled by fungal nutrition. To test this, we grew *A. luteobubalina* on different concentrations of PDA. We found that D-threitol was accumulated at high levels in fungal hyphae when grown on medium with lower levels of nutrition than the fungus grown on 1x PDA (Figure 6c). Therefore the nutritional status of the fungal colony impacts the synthesis of D-threitol.

3.5 | External treatment with threitol enhances microbial infection of *E. grandis* root tips

Given the fact that *Armillaria* produces threitol during the early stages of colonization, which coincides with the establishment phase of the fungus within the root system rather than the root damage phase (Figure 6a,b), we evaluated the effect of increased threitol levels upon the colonization ability of *A. luteobubalina* when in contact with *E. grandis* roots. Exogenous application of even very low levels of threitol enhanced root lesions caused by *A. luteobubalina*; a significant increase of ~10% and 25% by threitol treatment of 0.3 and 12 ppm, respectively, was observed (Figure 7a). To understand if this phenomenon was specific to *A. luteobubalina* colonization, or if the impact were more general, we also tested the impact of exogenous D-threitol application on the colonization by either *P. cinnamomi* or of *P. microcarpus*. We found that lesion development of roots colonized by *P. cinnamomi* was increased significantly when low amounts of D-threitol were supplied, but that this effect was reduced at higher levels of D-threitol (Figure 7b). Colonization of roots by the mutualistic fungus *P. microcarpus* was significantly enhanced at both levels of D-threitol tested (Figure 7c). Therefore, this metabolite signal can improve general microbial colonization of root tissues, although not as strongly as the impact on *A. luteobubalina* disease expression.

3.6 | External treatment with threitol alters transcription of hormone-responsive genes

As plant hormones are closely tied to colonization success of fungi (Chanclud & Morel, 2016), we sought to examine the transcriptional changes of a selection of hormone-responsive marker genes in *E. grandis* by qRT-PCR (Sarnowska et al., 2016). As shown in Figure 8a, threitol treatment significantly induced expression of all tested marker genes responsive to phytohormones including gibberellins, jasmonic acid, cytokinin, auxin, and abscisic acid. This was a surprising result given the fact that some of these pathways act in an antagonistic

TABLE 2 Performance index of the machine learning models used to select potential biomarkers for *Armillaria* infection in *Eucalyptus grandis*

		Performance index			Prediction performance index
Machine learning model	Optimized parameter	RMSE	R^2	Q^2	AUROC
parRF	mtry = 44	0.1965	0.9605	n.a.	1
rpart	cp = 0.1974	0.1373	0.9445	n.a.	0.9815
sPLSDA	keepX = 4, 4, 5; ncomp = 3	n.a.	0.9064	0.5493	0.8333

Abbreviations: AUROC, area under receiver operating characteristic; n.a., not applicable; RMSE, root mean square error.

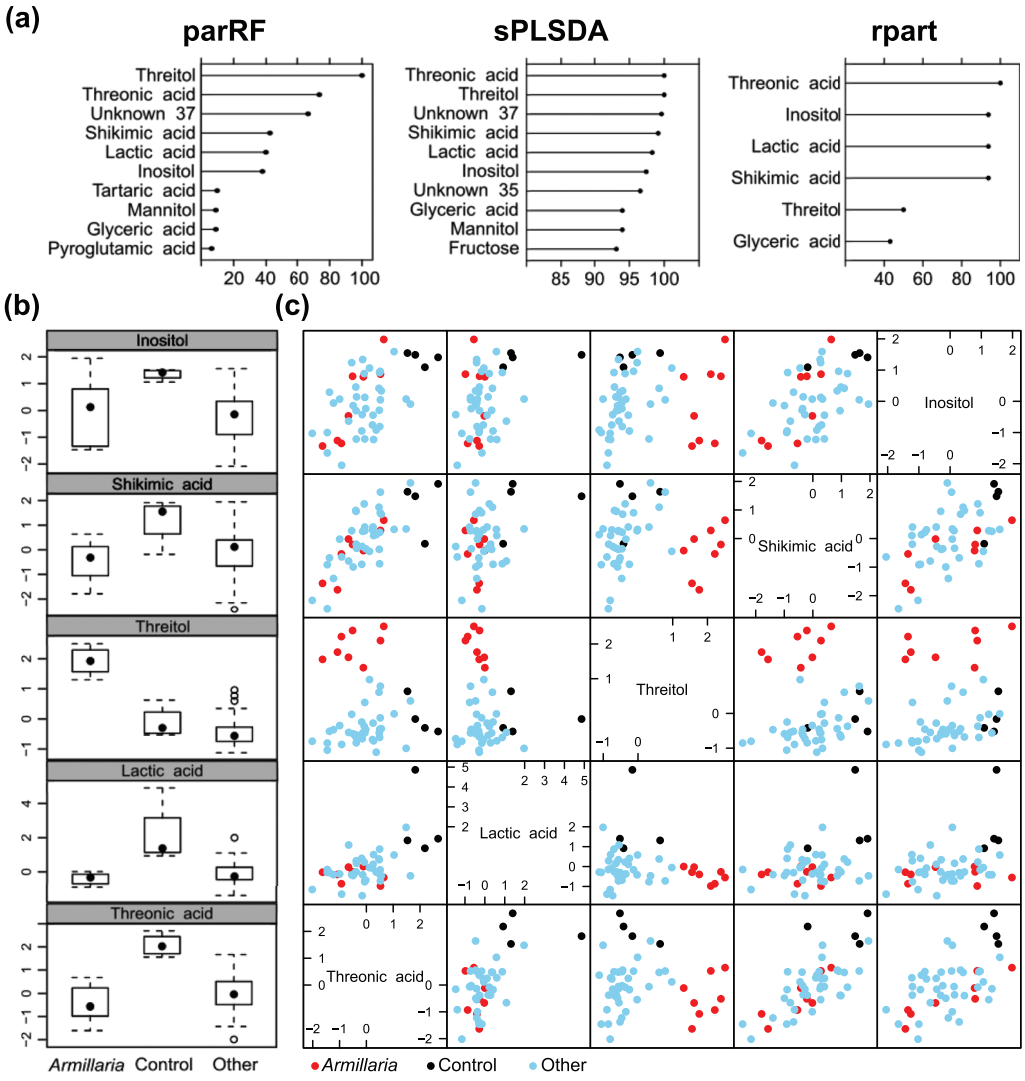

FIGURE 3 (a) The variable importance of the top 10 metabolite responses selected by three ML models. The variable importance is an indicator of the predictive power of the metabolite responses in discriminating between the three classifiers as follows: *Armillaria luteobubalina*-treated roots (*Armillaria*), untreated control roots (Control), and roots treated with other microbial species (Other). (b–c) The boxplot and scatter matrix plot showing the normalized metabolite responses of threonic acid, lactic acid, threitol, shikimic acid, and inositol across three classification groups. These five metabolite responses were commonly selected by all three MS models with the best predictive powers [Colour figure can be viewed at wileyonlinelibrary.com]

manner to each other. We, therefore, tested another one of the discriminatory metabolites from our profiling described above, myo-inositol, to determine if this response was just a stress response. We exposed the *E. grandis* root system to myo-inositol as we did for D-threitol and analysed expression of these same hormone responsive genes. In general, myo-inositol did not have any effect on the expression level of these genes with the exception of PIN2 (Figure 8b). Therefore, other metabolites found to be altered during the

TABLE 3 Unlabelled D-threitol quantitated with triple quadrupole gas chromatography-coupled mass spectrometry

Sample	Unlabelled D-threitol measured quantity (pmole/mg; *M ± SD*)
Root tips after 24-hr presymbiotic-contact with *Armillaria luteobubalina* growing in $^{12}C_6$-glucose media	126.3 ± 14.9
Root tips after 24-hr presymbiotic-contact with *A. luteobubalina* growing in $^{13}C_6$-glucose media	43.4 ± 12.6
Root tips after 24-hr presymbiotic-contact with *Pisolithus microcarpus* growing in $^{13}C_6$-glucose media	2.4 ± 2.8 [a]

[a]D-Threitol was measured to be below range for quantitation but within detection limit

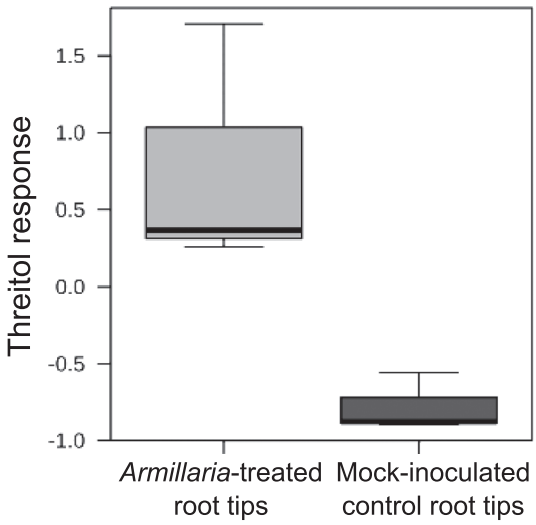

FIGURE 4 The threitol response of root tips towards *Armillaria luteobubalina* in pot soil-based sample in comparison with mock-inoculated control condition. The threitol response is normalized by dividing the detected peak corresponding to threitol by the weight of root tip samples, followed by log-transformation and auto-scaling. The difference in threitol response is significant with p value = .031

presymbiotic stage of *A. luteobubalina* disease progression have different impacts on plant signalling pathways.

4 | DISCUSSION

The metabolic regulation during plant–microbe interactions could be crucial in determining the outcome of the interaction (Buee, Rossignol, Jauneau, Ranjeva & Bécard, 2000; Akiyama, Matsuzaki & Hayashi, 2005; Steinkellner et al., 2007; Stuttmann et al., 2011; Lahrmann et al., 2013; Tschaplinski et al., 2014). *Armillaria* root rot is not only a widespread eucalypt tree disease endemic to Australia, but also a promiscuous root disease infecting numerous species of forest trees and crops worldwide (Baumgartner, Coetzee, & Hoffmeister, 2011). The *Armillaria* enzymatic activities contributing to its pathogenicity, as well as the plant metabolite responses towards *Armillaria* post-infection have previously been reported (Isidorov et al., 2008; Ross-Davis et al., 2013). However, our understanding on the "in plantae" molecular pathways initiating the *Armillaria*-plant interaction is still being developed and knowledge of specific metabolite profiles characteristic of *A. luteobubalina* pathogenicity are needed. In this study, we have demonstrated metabolite responses in eucalypt root tips as early as 24 hr after presymbiotic interaction with *A. luteobubalina*. Mannitol, threitol, and trehalose appear to be among the most significantly enriched metabolites in *A. luteobubalina*-treated roots. Whereas the role of threitol in plant-fungal interaction has not yet been reported, both mannitol and trehalose synthesis are known biotic stress responses of plants towards fungal attack (Fernandez, Béthencourt, Quero, Sangwan, & Clément, 2010; Patel & Williamson, 2016). Our findings suggest that these previously described metabolite responses of a plant host in response to fungal pathogens may be detectable after even very short periods of interaction with the pathogen, and that such regulation could be triggered solely by the exchange of metabolite signals without the need of physical contact.

Beyond their role in pathogenicity, metabolites have emerged as effective measures of plant performance and as biomarkers of disease during plant–microbe interactions (Fernandez et al., 2016; Sankaran, Mishra, Ehsani, & Davis, 2010). A good biomarker should

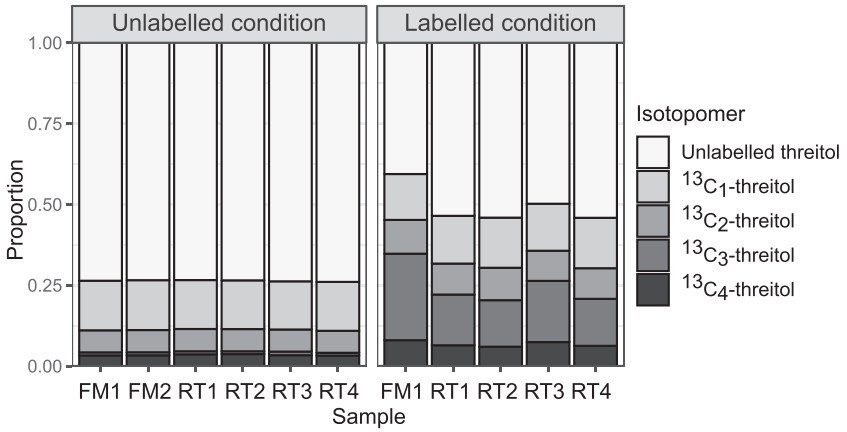

FIGURE 5 Distribution of different isotopomers of threitol detected across a set of *Armillaria luteobubalina* fungal mycelium samples (FM) and the interacting root tip samples (RT) in labelled and unlabeled control condition. The proportion of each isotopomer of threitol is calculated by dividing the detected intensity with the combined intensities of all detectable isotopomers. The shade of grey represent different isotopomers of derivatized threitol with distinct m/z values as follows: unlabeled threitol (m/z = 217), $^{13}C_1$-threitol (m/z = 218), $^{13}C_2$-threitol (m/z = 219), $^{13}C_3$-threitol (m/z = 220), and $^{13}C_4$-threitol (m/z = 221)

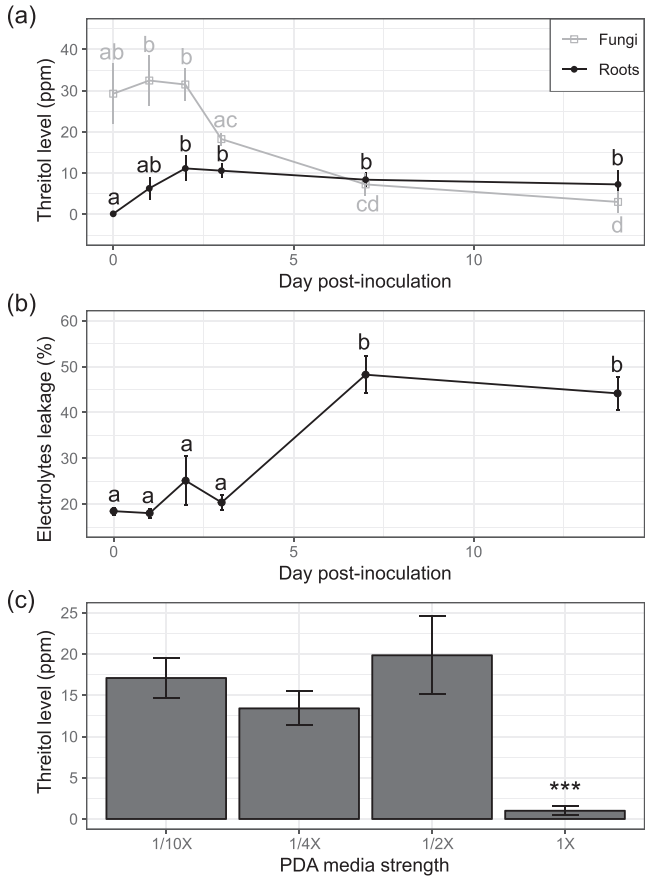

FIGURE 6 Quantification of threitol level (a) and cell damages as represented in form of electrolytes leakage (b) in *Eucalyptus grandis* root tissues (black line) and in *Armillaria luteobubalina* fungal mycelia tissues (grey line) over the time course of interaction. Threitol levels (ppm) are expressed as means ± standard error. Different letters indicate significant differences (p value < .05) among different time points. (c) Quantification of threitol level in *A. luteobubalina* fungal mycelia grown in PDA media of different strength. Asterisks indicate statistically significant differences (p value < .001, one-way analysis of variance). PDA, potato dextrose agar

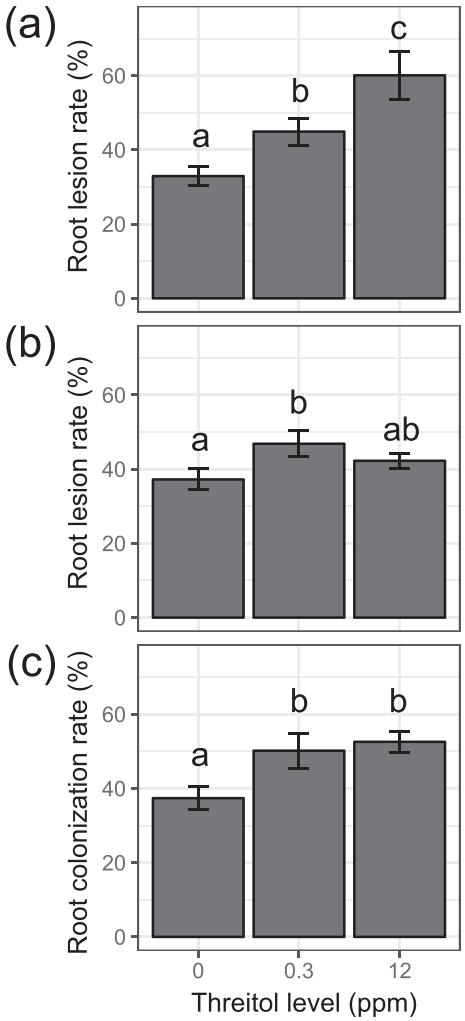

FIGURE 7 Effect of threitol enrichment at 0.3 and 12 ppm levels on the interaction of *Eucalyptus grandis* with different microbes. The bar-graphs depicts the percentage of root lesion caused by *Armillaria luteobubalina* (a) and *Phytophthora cinnamomi* (b), as well as the percentage of root colonization by *Pisolithus microcarpus* (c). Data points are means ± standard error. Different letters indicate significant differences (p value < .05) among different threitol levels.

achieve both high sensitivity and specificity for robust indication of the plant disease (Nagana Gowda & Raftery, 2013). Studying the specificity of plant metabolite responses could thus benefit both our basic knowledge of *Armillaria* disease and also the development of biomarkers for its early detection. In this study, not only have we identified the early metabolite responses of *E. grandis* towards *A. luteobubalina* prior to infection, but these metabolite profiles were also compared with roots exposed to representatives of fungi from other lifestyles—mutualist (*P. microcarpus*), "commensalist" (*S. granulatus*), and hemi-biotrophic pathogen (*P. cinnamomi*) under the exact same conditions. Our results showed that the overall metabolite profiles of eucalypt roots after different microbial presymbiotic treatment was highly-overlapping, suggesting that there are common innate metabolite responses common to this very early stage of interaction regardless of the microbial species present. This observation is aligned with a study by Müller et al. (2013), which showed a large number of common volatile organic compounds emitted by both ectomycorrhizal fungi, pathogenic fungi, and saprophytic fungi. To separate metabolite responses specific towards *A. luteobubalina* from common responses towards other microbial species, we employed an emerging tool for selection of important features in metabolomic studies—machine learning models (Poezevara et al., 2017; Shiokawa, Date, & Kikuchi, 2018). The three ML models used in this study were able to identify a panel of important features that differentiate root metabolite responses of the *Armillaria* interaction from other microbial interactions or the axenically grown control plant. We have selected threitol among the important features for further characterization as it is strongly induced in the *Armillaria* interaction. It is possible that additional untargeted metabolomic methods (e.g., liquid chromatography with tandem mass spectrometry) would identify further lifestyle or fungal-specific metabolite signals, but our work stands as a proof of concept that we can use even the simplified approach of standard GC-MS analysis for

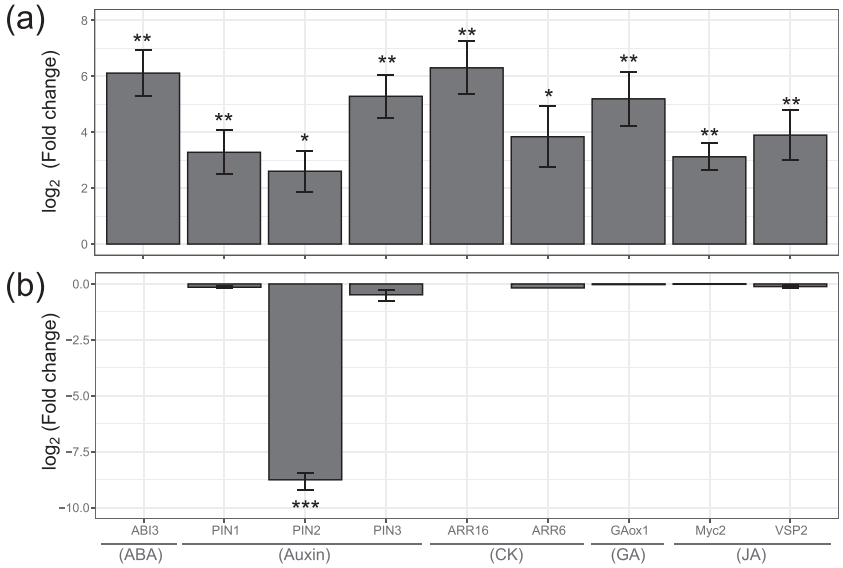

FIGURE 8 Fold change corresponding to the expression of nine marker genes responsive towards different hormones (shown in bracket) in *Eucalyptus grandis* roots after 1-day exposure to threitol (a) and to inositol (b). Fold changes of these genes are $\log_2$-transformed and shown in comparison to 0 ppm control condition. Data points are means ± standard error. Asterisk (*) above the bars indicate the significance of the gene expression changes in relation to the 0 ppm control condition (*p value < .05, **p value < .01, ***p value < .001). ABA, abscisic acid; CK, cytokinin; GA, gibberellins; JA, jasmonic acid

identifying specific metabolites that are linked to root colonization by a specific pathogen. Given that our comparative approach has taken the interaction of a host with microbial species of other lifestyles into consideration, these current results indicate that threitol is a promising biomarker specific for *Armillaria* infection of *E. grandis* roots.

Threitol, a four-carbon sugar alcohol, has been detected in plant species such as *Nicotiana tabacum* and *Coffea arabica*, as well as in mycelia of *Armillaria* fungal species (Birkinshaw, Stickings, & Tessier, 1948; Hacham, Matityahu, & Amir, 2017; Martins, Araújo, Tohge, Fernie, & DaMatta, 2014). Hence, it was unclear whether the threitol detected in the *E. grandis* roots with the current study was derived from the fungal pathogen or the *E. grandis* itself. By determining the isotopic composition of threitol in *E. grandis* root tissue after interaction with ^{13}C-labelled *A. luteobubalina*, we identified that threitol detected in root tissues were ^{13}C-enriched—meaning that it is chiefly secreted by *A. luteobubalina* and translocated to *E. grandis* root tissues. This conclusion was further reinforced when comparing the relative concentration differences of D-threitol in between *A. luteobubalina* and *E. grandis* across all of the colonization time course (Figure 6). Specifically, D-threitol levels in the roots followed fungal production levels, albeit at a lower concentration than in fungal tissues. It is also interesting to note that fungal production of D-threitol may be nutritionally regulated. In both culturing conditions and during the stage when *A. luteobubalina* would be recovering nutrients from its host (i.e., >48 hr when ion leakage increases), we observe that D-threitol production decreases. Therefore, this is not only a signal produced by *A. luteobubalina*, but it is perhaps also related to enhancing nutrient acquisition by the fungus.

The function and metabolic pathway of threitol in either plants or fungi remain obscure despite being a natural product of both. Therefore, it is currently impossible to follow the transcriptomic expression patterns of threitol-related biosynthetic genes nor to make fungal mutants that produce less threitol. Threitol was found to be a derivative of sorbose in plants (McComb & Rendig, 1963), a stereoisomer of erythritol in *Armillaria mellea* (Birkinshaw et al., 1948), and a precursor of erythrulose and erythrose in bacteria *Mycobacterium smegmatis* (Huang et al., 2015). The effect of fungal-derived threitol on plant roots has hitherto been undescribed. We have tested the effect of threitol on hormonal responses and microbial colonization in *E. grandis*. Our findings indicate induced expression of hormone-responsive genes in roots towards gibberellins, jasmonic acid, cytokinin, auxin, and abscisic acid upon threitol treatment, an effect that was not observed when myo-inositol; one of the other *Armillaria*-specific metabolites was also exposed to *E. grandis* roots. In spite of its large impact of a wide range of hormonal pathways in the plant, colonization of *A. luteobubalina* appears to be favoured by exogenous threitol treatment. This colonization promotion was also observed to a lesser extent when *E. grandis* was placed into contact with either *P. cinnamomi* or *P. microcarpus*. These results suggest that, whereas threitol may be produced by *A. luteobubalina* to foster colonization, this metabolite may alter plant immunity in general way that can benefit more than just *Armillaria* colonization. More research on the specific mechanism of threitol's action during plant–microbe interactions will be necessary in future.

Our study has advanced our understanding of the presymbiotic metabolite regulation in *E. grandis* prior to infection by *A. luteobubalina*. We identified threitol enrichment as an important early stage metabolite in the *Armillaria*-induced response and highlighted the potential of threitol as a biomarker for *Armillaria* disease detection. In addition, our study provides insight into the promotional effect of threitol on root colonization by varying microbes in *E. grandis*. Given that *Armillaria* species are found in major forest ecosystems globally, further investigation should follow to better our understanding of the role of their metabolites in pathogenicity and soil ecology.

ACKNOWLEDGEMENTS

J.W. would like to acknowledge the Western Sydney University for a PhD research scholarship and the North Shore District Group of the Australian Plants Society for the Valette Williams Scholarship in Botany to support this research project. J.P. would like to acknowledge the Australian Research Council for research funding (DE150100408). We would also thank J.Rigg, E.Liew, and M.Laurence of the Botanic Gardens & Centennial Parklands for providing isolates of *A. luteobubalina* and *P. cinnamomi* and S.Hortal for providing isolates of *A. luteobubalina* and *S. granulatus*. The metabolite analyses were conducted at Metabolomics Australia (School of BioSciences, The University of Melbourne, Australia), a National Collaborative Research Infrastructure Strategy initiative under Bioplatforms Australia Pty Ltd. We would like to acknowledge V.Liu, K.Kwan, H.Mendis, and N. Jayasinghe from the Metabolomics Australia for their contribution on the metabolite analyses involved in this study.

CONFLICT OF INTEREST

The authors declare that they have no conflict of interest.

ORCID

Johanna W.-H. Wong https://orcid.org/0000-0001-6119-8645
Krista L. Plett https://orcid.org/0000-0001-6422-3754
Ute Roessner https://orcid.org/0000-0002-6482-2615
Jonathan M. Plett https://orcid.org/0000-0003-0514-8146

REFERENCES

Akiyama, K., Matsuzaki, K., & Hayashi, H. (2005). Plant sesquiterpenes induce hyphal branching in arbuscular mycorrhizal fungi. *Nature*, *435* (7043, 824–827. https://doi.org/10.1038/nature03608

Baumgartner, K., Coetzee, M. P. A., & Hoffmeister, D. (2011). Secrets of the subterranean pathosystem of *Armillaria*. *Molecular Plant Pathology*, *12*, 515–534. https://doi.org/10.1111/j.1364-3703.2010.00693.x

Beguiristain, T., & Lapeyrie, F. (1997). Host plant stimulates hypaphorine accumulation in *Pisolithus tinctorius* hyphae during ectomycorrhizal infection while excreted fungal hypaphorine controls root hair development. *New Phytologist*, *136*, 525–532.

Birkinshaw, J. H., Stickings, C. E., & Tessier, P. (1948). Biochemistry of the wood-rotting fungi: 5. The production of d-threitol (l-erythritol) by *Armillaria mellea* (Vahl) Quélet. *Biochemical Journal*, *42*, 329–332. https://doi.org/10.1042/bj0420329

Buee, M., Rossignol, M., Jauneau, A., Ranjeva, R., & Bécard, G. (2000). The Pre-Symbiotic Growth of Arbuscular Mycorrhizal Fungi Is Induced by a Branching Factor Partially Purified from Plant Root Exudates. *Molecular Plant-Microbe Interactions*, *13*(6, 693–698. https://doi.org/10.1094/mpmi.2000.13.6.693

Burgess, T., & Wingfield, M. J. (2004). Impact of fungal pathogens in natural forest ecosystems: A focus on eucalypts. In K. Sivasithamparama, K. W. Dixon, & R. L. Barrett (Eds.), *Microorganisms in plant conservation and biodiversity* (pp. 285–306). Dordrecht: Kluwer Academic Publishers.

Chanclud, E., & Morel, J.-B. (2016). Plant hormones: A fungal point of view. *Molecular Plant Pathology*, *17*, 1289–1297. https://doi.org/10.1111/mpp.12393

Collins, C., Keane, T. T. M., Turner, D. J., O'Keeffe, G., Fitzpatrick, D. A., & Doyle, S. (2013). Genomic and proteomic dissection of the ubiquitous plant pathogen, *Armillaria mellea*: Toward a new infection model system. *Journal of Proteome Research*, *12*, 2552–2570. https://doi.org/10.1021/pr301131t

Dias, D. A., Hill, C. B., Jayasinghe, N. S., Atieno, J., Sutton, T., & Roessner, U. (2015). Quantitative profiling of polar primary metabolites of two chickpea cultivars with contrasting responses to salinity. *Journal of Chromatography B*, *1000*, 1–13. https://doi.org/10.1016/j.jchromb.2015.07.002

Fernandez, O., Béthencourt, L., Quero, A., Sangwan, R. S., & Clément, C. (2010). Trehalose and plant stress responses: Friend or foe? *Trends in Plant Science*, *15*, 409–417. https://doi.org/10.1016/j.tplants.2010.04.004

Fernandez, O., Urrutia, M., Bernillon, S., Giauffret, C., Tardieu, F., Le Gouis, J., … Gibon, Y. (2016). Fortune telling: Metabolic markers of plant performance. *Metabolomics*, *12*, 158. https://doi.org/10.1007/s11306-016-1099-1

Guo, J., McCulley, R. L., & McNear, D. H. J. (2015). Tall fescue cultivar and fungal endophyte combinations influence plant growth and root exudate composition. *Frontiers in Plant Science*, *6*. https://doi.org/10.3389/fpls.2015.00183

Hacham, Y., Matityahu, I., & Amir, R. (2017). Transgenic tobacco plants having a higher level of methionine are more sensitive to oxidative stress. *Physiologia Plantarum*, *160*, 242–252. https://doi.org/10.1111/ppl.12557

Huang, H., Carter, M. S., Vetting, M. W., Al-Obaidi, N., Patskovsky, Y., Almo, S. C., & Gerlt, J. A. (2015). A general strategy for the discovery of metabolic pathways: D-Threitol, l-threitol, and erythritol utilization in *Mycobacterium smegmatis*. *Journal of the American Chemical Society*, *137*, 14570–14573. https://doi.org/10.1021/jacs.5b08968

Isidorov, V. A., Lech, P., Żółciak, A., Rusak, M., & Szczepaniak, L. (2008). Gas chromatographic–mass spectrometric investigation of metabolites from the needles and roots of pine seedlings at early stages of pathogenic fungi *Armillaria ostoyae* attack. *Trees*, *22*, 531–542. https://doi.org/10.1007/s00468-008-0213-z

Kamilova, F., Kravchenko, L. V., Shaposhnikov, A. I., Makarova, N., & Lugtenberg, B. (2006). Effects of the tomato pathogen *Fusarium oxysporum* f. sp. radicis-lycopersici and of the biocontrol bacterium *Pseudomonas fluorescens* WCS365 on the composition of organic acids and sugars in tomato root exudate. *Molecular Plant-Microbe Interactions*, *19*, 1121–1126. https://doi.org/10.1094/MPMI-19-1121

Kile, G. A. (1981). *Armillaria luteobubalina* a primary cause of decline and death of trees in mixed species eucalypt forests in central Victoria. *Australian Forest Research*, *11*, 63–77.

Kile, G. A. (2000). Woody root rots of eucalypts. In P. J. Kean, G. A. Kile, F. D. Podger, & B. N. Brown (Eds.), *Diseases and pathogens of eucalypts* (pp. 293–306). Australia: CSIRO publishing.

Lahrmann, U., Ding, Y., Banhara, A., Rath, M., Hajirezaei, M. R., Döhlemann, S., … Zuccaro, A. (2013). Host-related metabolic cues affect colonization strategies of a root endophyte. *Proceedings of the National Academy of Sciences*, *110*, 13965–13970. https://doi.org/10.1073/pnas.1301653110

Martins, S. C. V., Araújo, W. L., Tohge, T., Fernie, A. R., & DaMatta, F. M. (2014). In high-light-acclimated coffee plants the metabolic machinery is adjusted to avoid oxidative stress rather than to benefit from extra light enhancement in photosynthetic yield. *PLoS ONE*, *9*, e94862. https://doi.org/10.1371/journal.pone.0094862

McComb, E. A., & Rendig, V. V. (1963). Isolation and identification of L-threitol from plants fed L-sorbose. *Archives of Biochemistry and Biophysics*, *103*, 84–86. https://doi.org/10.1016/0003-9861(63)90012-2

Müller, A., Faubert, P., Hagen, M., zu Castell, W., Polle, A., Schnitzler, J.-P., & Rosenkranz, M. (2013). Volatile profiles of fungi—Chemotyping of species and ecological functions. *Fungal Genetics and Biology*, *54*, 25–33. https://doi.org/10.1016/j.fgb.2013.02.005

Nagana Gowda, G. A., & Raftery, D. (2013). Biomarker discovery and translation in metabolomics. *Current Metabolomics*, *1*, 227–240. https://doi.org/10.2174/2213235X113019990005

Nanchen, A., Fuhrer, T., & Sauer, U. (2007). Determination of metabolic flux ratios from 13C-experiments and gas chromatography-mass spectrometry data: Protocol and principles. *Methods in Molecular Biology (Clifton, N. J.)*, *358*, 177–197. https://doi.org/10.1007/978-1-59745-244-1_11

Nusaibah, S. A., Siti Nor Akmar, A., Idris, A. S., Sariah, M., & Mohamad, P. Z. (2016). Involvement of metabolites in early defense mechanism of oil palm (*Elaeis guineensis* Jacq.) against Ganoderma disease. *Plant Physiology and Biochemistry*, *109*, 156–165. https://doi.org/10.1016/j.plaphy.2016.09.014

Patel, T. K., & Williamson, J. D. (2016). Mannitol in plants, fungi, and plant–fungal interactions. *Trends in Plant Science*, *21*, 486–497. https://doi.org/10.1016/j.tplants.2016.01.006

Poezevara, G., Lozano, S., Cuissart, B., Bureau, R., Bureau, P., Croixmarie, V., … Lepailleur, A. (2017). A computational selection of metabolite biomarkers using emerging pattern mining: A case study in human hepatocellular carcinoma. *Journal of Proteome Research*, *16*, 2240–2249. https://doi.org/10.1021/acs.jproteome.7b00054

Robinson, R. M. (2003). Short-term impact of thinning and fertilizer application on *Armillaria* root disease in regrowth karri (*Eucalyptus diversicolor* F. Muell.) in Western Australia. *Forest Ecology and Management*, *176*, 417–426.

Roessner, U., Luedemann, A., Brust, D., Fiehn, O., Linke, T., Willmitzer, L., & Fernie, A. R. (2001). Metabolic profiling allows comprehensive phenotyping of genetically or environmentally modified plant systems. *The Plant Cell*, *13*, 11–29. https://doi.org/10.1105/tpc.13.1.11

Ross-Davis, A. L., Stewart, J. E., Hanna, J. W., Kim, M.-S., Knaus, B. J., Cronn, R., … Klopfenstein, N. B. (2013). Transcriptome of an *Armillaria* root disease pathogen reveals candidate genes involved in host substrate utilization at the host–pathogen interface. *Forest Pathology*, *43*, 468–477. https://doi.org/10.1111/efp.12056

Sade, D., Shriki, O., Cuadros-Inostroza, A., Tohge, T., Semel, Y., Haviv, Y., … Brotman, Y. (2014). Comparative metabolomics and transcriptomics of plant response to Tomato yellow leaf curl virus. *Metabolomics*, *11*, 81–97.

Sankaran, S., Mishra, A., Ehsani, R., & Davis, C. (2010). A review of advanced techniques for detecting plant diseases. *Computers and Electronics in Agriculture*, *72*, 1–13.

Sarnowska, E., Gratkowska, D. M., Sacharowski, S. P., Cwiek, P., Tohge, T., Fernie, A. R., … Sarnowski, T. J. (2016). The role of SWI/SNF chromatin remodeling complexes in hormone crosstalk. *Trends in Plant Science*, *21*, 594–608. https://doi.org/10.1016/j.tplants.2016.01.017

Scalbert, A., Brennan, L., Fiehn, O., Hankemeier, T., Kristal, B. S., van Ommen, B., … Wopereis, S. (2009). Mass-spectrometry-based metabolomics: Limitations and recommendations for future progress with particular focus on nutrition research. *Metabolomics*, *5*, 435–458. https://doi.org/10.1007/s11306-009-0168-0

Sherif, M., Becker, E.-M., Herrfurth, C., Feussner, I., Karlovsky, P., & Splivallo, R. (2016). Volatiles emitted from maize ears simultaneously infected with two *Fusarium* species, mirror the most competitive fungal pathogen. *Frontiers in Plant Science*, *7*. https://doi.org/10.3389/fpls.2016.01460

Shiokawa, Y., Date, Y., & Kikuchi, J. (2018). Application of kernel principal component analysis and computational machine learning to exploration of metabolites strongly associated with diet. *Scientific Reports*, *8*, 3426. https://doi.org/10.1038/s41598-018-20121-w

Steinkellner, S., Lendzemo, V., Langer, I., Schweiger, P., Khaosaad, T., Toussaint, J.-P., & Vierheilig, H. (2007). Flavonoids and Strigolactones in Root Exudates as Signals in Symbiotic and Pathogenic Plant-Fungus Interactions. *Molecules*, *12*(7), 1290–1306. https://doi.org/10.3390/12071290

Sturrock, R. N., Frankel, S. J., Brown, A. V., Hennon, P. E., Kliejunas, J. T., Lewis, K. J., … Woods, A. J. (2011). Climate change and forest diseases. *Plant Pathology*, *60*, 133–149. https://doi.org/10.1111/j.1365-3059.2010.02406.x

Stuttmann, J., Hubberten, H.-M., Rietz, S., Kaur, J., Muskett, P., Guerois, R., … Parker, J. E. (2011). Perturbation of arabidopsis amino acid metabolism causes incompatibility with the adapted biotrophic pathogen *Hyaloperonospora arabidopsidis*. *The Plant Cell*, *23*, 2788–2803. https://doi.org/10.1105/tpc.111.087684

Tschaplinski, T. J., Plett, J. M., Engle, N. L., Deveau, A., Cushman, K. C., Martin, M. Z., … Martin, F. (2014). *Populus trichocarpa* and *Populus deltoides* exhibit different metabolomic responses to colonization by the symbiotic fungus *Laccaria bicolor*. *Molecular Plant-Microbe Interactions*, *27*, 546–556. https://doi.org/10.1094/MPMI-09-13-0286-R

Vinaixa, M., Schymanski, E. L., Neumann, S., Navarro, M., Salek, R. M., & Yanes, O. (2016). Mass spectral databases for LC/MS- and GC/MS-based metabolomics: State of the field and future prospects. *TrAC Trends in Analytical Chemistry*, *78*, 23–35. https://doi.org/10.1016/j.trac.2015.09.005

Wong, J. W.-H., Lutz, A., Natera, S., Wang, M., Ng, V., Grigoriev, I. V., … Plett, J. M. (2019). The influence of contrasting microbial lifestyles on the pre-symbiotic metabolite responses of *Eucalyptus grandis* roots. *Frontiers in Ecology and Evolution*, *7*, 10. https://doi.org/10.3389/fevo.2019.00010

Xu, X. H., Wang, C., Li, S. X., Su, Z. Z., Zhou, H. N., Mao, L. J., … Kubicek, C. P. (2015). Friend or foe: differential responses of rice to invasion by mutualistic or pathogenic fungi revealed by RNAseq and metabolite profiling. *Scientific Reports*, *5*, 13624.

SUPPORTING INFORMATION

Additional supporting information may be found online in the Supporting Information section at the end of the article.

How to cite this article: Wong JW-H, Plett KL, Natera SHA, Roessner U, Anderson IC, Plett JM. Comparative metabolomics implicates threitol as a fungal signal supporting colonization of *Armillaria luteobubalina* on eucalypt roots. *Plant Cell Environ*. 2019;1–13. https://doi.org/10.1111/pce.13672